ISSN 1674-1056
http://cpb.iphy.ac.cn
http://iopscience.iop.org/cpb
中国物理 B
Chinese Physics
中国物理 Chinese Physics B

A novel diluted magnetic semiconductor (Ca,Na)(Zn,Mn)$_2$Sb$_2$ with decoupled charge and spin dopings

Yilun Gu(顾轶伦), Haojie Zhang(张浩杰), Rufei Zhang(张茹菲), Licheng Fu(傅立承), Kai Wang(王恺), Guoxiang Zhi(智国翔), Shengli Guo(郭胜利), Fanlong Ning(宁凡龙)
Citation: Chin. Phys. B . 2020, 29(5): 057507 . **doi:** 10.1088/1674-1056/ab892e
Journal homepage: http://cpb.iphy.ac.cn; http://iopscience.iop.org/cpb

What follows is a list of articles you may be interested in

Effects of chemical pressure on diluted magnetic semiconductor (Ba,K)(Zn,Mn)$_2$As$_2$

Y Peng(彭毅), S Yu(于爽), G Q Zhao(赵国强), W M Li(李文敏), J F Zhao(赵建发), L P Cao(曹立朋), X C Wang(望贤成), Q Q Liu(刘清青), S J Zhang(张思佳), R Z Yu(于润泽), Z Deng(邓正), X H Zhu(朱小红), C Q Jin(靳常青)
Chin. Phys. B . 2019, 28(5): 057501 . **doi:** 10.1088/1674-1056/28/5/057501

Magnetic properties of Sn-substituted Ni–Zn ferrites synthesized from nano-sized powders of NiO, ZnO, Fe_2O_3, and SnO_2

M A Ali, M M Uddin, M N I Khan, F U Z Chowdhury, S M Hoque, S I Liba
Chin. Phys. B . 2017, 26(7): 077501 . **doi:** 10.1088/1674-1056/26/7/077501

Magnetic entropy change and magnetic properties of LaFe$_{11.5}$Si$_{1.5}$ after controlling the Curie temperature by partial substitution of Mn and hydrogenation

Bin Fu(傅斌) and Jie Han(韩洁)
Chin. Phys. B . 2016, 25(2): 027501 . **doi:** 10.1088/1674-1056/25/2/027501

Structural and magnetic properties of $La_{0.7}Sr_{0.1}Ag_xMnO_{3-\delta}$ perovskite manganites

Hou Xue, Ji Deng-Hui, Qi Wei-Hua, Tang Gui-De, Li Zhuang-Zhi
Chin. Phys. B . 2015, 24(5): 057501 . **doi:** 10.1088/1674-1056/24/5/057501

Influence of the Jahn–Teller distortion on magnetic ordering in $TbMn_{1-x}Fe_xO_3$

Jin Jin-Ling, Zhang Xiang-Qun, Li Guo-Ke, Cheng Zhao-Hua
Chin. Phys. B . 2012, 21(10): 107501 . **doi:** 10.1088/1674-1056/21/10/107501

A novel diluted magnetic semiconductor (Ca,Na)(Zn,Mn)$_2$Sb$_2$ with decoupled charge and spin dopings*

Yilun Gu(顾轶伦)[1], Haojie Zhang(张浩杰)[1], Rufei Zhang(张茹菲)[1], Licheng Fu(傅立承)[1], Kai Wang(王恺)[1], Guoxiang Zhi(智国翔)[1], Shengli Guo(郭胜利)[1], and Fanlong Ning(宁凡龙)[1,2,†]

[1] *Zhejiang Province Key Laboratory of Quantum Technology and Device and Department of Physics, Zhejiang University, Hangzhou* 310027, *China*
[2] *Collaborative Innovation Center of Advanced Microstructures, Nanjing University, Nanjing* 210093, *China*

(Received 8 March 2020; revised manuscript received 14 April 2020; accepted manuscript online 15 April 2020)

We report the successful synthesis of a new diluted magnetic semiconductor (Ca,Na)(Zn,Mn)$_2$Sb$_2$. Na and Mn are doped into the parent compound CaZn$_2$Sb$_2$, which has the same crystal structure as that of "122" type iron-based superconductor CaFe$_2$As$_2$. Na substitution for Ca and Mn substitution for Zn introduce carriers and spins, respectively. Doping Mn atoms alone up to 5% does not induce any type of magnetic ordering. When both Na and Mn are co-doped, a ferromagnetic ordering with maximum $T_C \sim 10$ K has been observed. Iso-thermal magnetization shows that the coercive field is up to ~ 245 Oe at 2 K. Below T_C, a negative magneto-resistance with MR $\sim 12\%$ has also been achieved.

Keywords: CaZn$_2$Sb$_2$, magnetic ordering, Curie temperature

PACS: 75.50.Pp, 75.50.Dd, 75.30.Kz **DOI:** 10.1088/1674-1056/ab892e

1. Introduction

The successful fabrication of (Ga,Mn)As films has attracted a lot of attention in the research of diluted magnetic semiconductors (DMSs).[1–5] However, the substitution of Mn for Ga induces both spin and charge dopings, which makes it difficult to control the spin and carrier densities separately. On the other hand, the maximum T_C of (Ga,Mn)As is only 200 K,[6] which is still below the room temperature that is the requirement for practical applications. Recently, a series of new bulk form DMSs with decoupled charge and spin dopings have been reported.[7–9] According to the crystal structure, they are classified as 111-type Li(Zn,Mn)As,[10] Li(Zn,Mn)P,[11] 122-type (Ba,K)(Zn,Mn)$_2$As$_2$,[12] (Ca,Na)(Zn,Mn)$_2$As$_2$,[13] and 1111-type (La,Ba)(Zn,Mn)AsO,[14] (La,Sr)(Zn,Mn)AsO,[15] La(Zn,Mn,Cu)SbO,[16] etc. In these new DMSs, spins are introduced by the substitution of Mn^{2+} for Zn^{2+}, and carriers can be introduced at a different site, which enables the investigation of how the carrier or spin density affects T_C. Further more, muon spin rotation (μSR) measurements have demonstrated that these DMSs have the same ferromagnetic mechanism as that of (Ga,Mn)As.[17,18] Investigation of these bulk form DMSs will therefore help to understand the common ferromagnetism in all diluted magnetic systems.

Among these novel DMSs, 122-type DMSs have been extensively studied. The Curie temperature T_C of 122-type (Ba,K)(Zn,Mn)$_2$As$_2$ has reached ~ 230 K.[19] Very recently, a 122-type DMS Ba(Zn,Co)$_2$As$_2$ with n-type carriers and $T_C \sim 45$ K has been reported.[20] The 122-type series of DMSs do not have the same crystal structure. For example, (Ca,Na)(Zn,Mn)$_2$As$_2$[13] has a hexagonal CaAl$_2$Si$_2$ structure, while (Ba,K)(Zn,Mn)$_2$As$_2$ has a tetragonal ThCr$_2$Si$_2$ structure,[12] and (Ba,K)(Cu,Mn)$_2$Se$_2$ has an orthorhombic BaCu$_2$S$_2$ structure.[21] In this paper, we report the successful synthesis of a new 122 DMS (Ca,Na)(Zn,Mn)$_2$Sb$_2$ through the doping of Na and Mn into a hexagonal crystal CaZn$_2$Sb$_2$. CaZn$_2$Sb$_2$ has been known as nonmagnetic with small energy gap.[22] We find that co-doping Na and Mn into CaZn$_2$Sb$_2$ induces a ferromagnetic ordering with a maximum $T_C \sim 10$ K. Our work represents a new member of DMS families.

2. Experiments

Polycrystalline samples of $(Ca_{1-x}Na_x)(Zn_{2-x}Mn_x)Sb_2$ were synthesised through solid-state reaction method. High purity elements of Ca, Na, Zn, Mn, and Sb were mixed, pressed into pellets, and heated at 200 °C for 10 h in evacuated silica tubes. The mixture was then heated at 750 °C for 40 h before cooling to room temperature at a rate of 10 °C/h. The crystal structure was characterized via powder x-ray diffraction (XRD) at room temperature with a powder x-ray diffractometer (Model EMPYREAN) using monochromatic Cu $K_{\alpha 1}$ radiation. The DC magnetization measurements were conducted on a Quantum Design magnetic property measurement system. The resistivity was measured via the typical four-probe method, and the magneto-resistance was measured by a physical property measurement system.

*Project supported by the National Key Research & Development Program of China (Grant No. 2016YFA0300402) and the Fundamental Research Funds for the Central Universities, China.

†Corresponding author. E-mail: ningfl@zju.edu.cn

© 2020 Chinese Physical Society and IOP Publishing Ltd

3. Results and discussion

In Fig. 1(a), we show the x-ray diffraction patterns for $(Ca_{1-x}Na_x)(Zn_{2-x}Mn_x)Sb_2$ ($x = 0.08, 0.10, 0.12, 0.16, 0.20$). The XRD patterns of the samples can be well indexed by a $CaAl_2Si_2$-type hexagonal crystal structure which is shown in the inset of Fig. 1(b). Some traces of ZnSb and Sb impurities were observed in the samples and marked as triangles and stars. They are both paramagnetic and have no influences on the ferromagnetic behaviors discussed in the following. In Fig. 1(b), we show the Rietveld refinement for $(Ca_{0.88}Na_{0.12})(Zn_{1.88}Mn_{0.12})Sb_2$ by GSAS-II.[23] The resultant weighted reliable factor is 9.8%, indicating that this sample has a good quality. From the Rietveld refinement structural analysis, we obtain the lattice parameter c and plot it in Fig. 1(c). The lattice parameter c monotonically increases from 7.478 Å for $x = 0.08$ to 7.499 Å for $x = 0.20$, indicating the successful doping of Na and Mn. The synthesis of the sample with higher doping level of $x > 0.20$ was not successful and some secondary phase started to appear, which suggests that the chemical solubility in $(Ca_{1-x}Na_x)(Zn_{2-x}Mn_x)Sb_2$ is 20%.

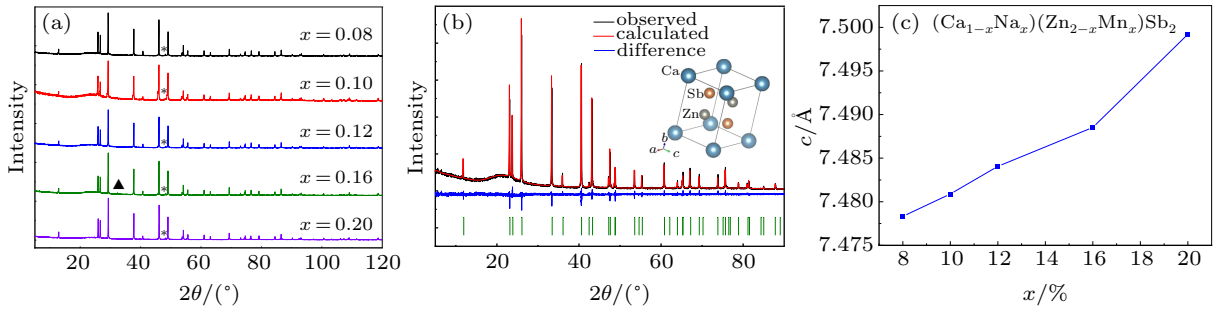


Fig. 1. (a) The XRD patterns for $(Ca_{1-x}Na_x)(Zn_{2-x}Mn_x)Sb_2$ ($x = 0.08, 0.10, 0.12, 0.16, 0.20$). Traces of impurities ZnSb (*) and Sb (▲) are marked. (b) The Rietveld refinement of $(Ca_{0.88}Na_{0.12})(Zn_{1.88}Mn_{0.12})Sb_2$. Inset is the crystal structure of $CaZn_2Sb_2$. (c) The lattice parameter c of $(Ca_{1-x}Na_x)(Zn_{2-x}Mn_x)Sb_2$.

In Fig. 2, we show the temperature dependent magnetization of $Ca(Zn_{1.9}Mn_{0.1})Sb_2$ measured under field-cooled conditions with an external field $B_{ext} \sim 100$ Oe. No magnetic ordering is observed below 150 K, indicating that doping Mn only will not induce any type of magnetic ordering. We plot $1/(M - M_0)$ versus temperature as the inset of Fig. 2. It is a straight line. This result is consistent with that of previously reported 1111-type and 122-type DMSs.[12,14] That is, Mn substitution for Zn without carriers will not induce any type of magnetic ordering.

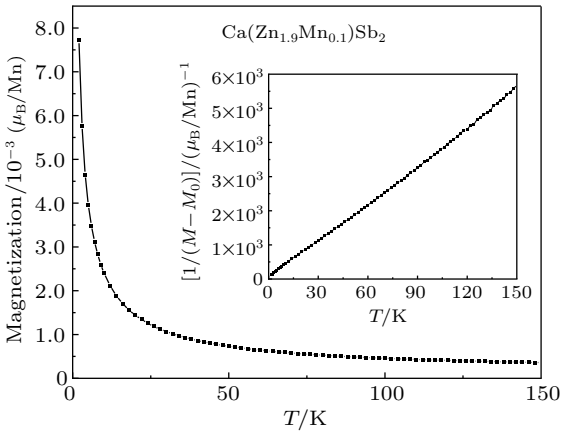


Fig. 2. The temperature dependence of the DC magnetization for $Ca(Zn_{1.9}Mn_{0.1})Sb_2$ measured under field-cooling (FC) with external field of 100 Oe. Inset: the plot of $1/(M - M_0)$ versus temperature.

In Fig. 3(a), we show the temperature dependent magnetization of $(Ca_{1-x}Na_x)(Zn_{2-x}Mn_x)Sb_2$ ($x = 0.08, 0.10, 0.12, 0.16, 0.20$) measured under field-cooled conditions with an external field $B_{ext} \sim 1000$ Oe. We can see that below $T \sim 20$ K, the magnetization starts to increase abruptly. The saturation moments at the base temperature of 2 K decrease from 1.06 μ_B/Mn for $x = 0.08$ to 0.56 μ_B/Mn for $x = 0.20$. This is caused by the increase of the nearest-neighbour (NN) Mn-Mn antiferromagnetic interaction. The probability of finding two Mn atoms at NN Zn site is $C_4^1(x/2)(1-x/2)^3 = 14.16\%$ for $x = 0.08$ and increases to 29.16% for $x = 0.20$. We plot the first derivative of magnetization versus temperature in Fig. 3(b). The Curie temperature is defined as the minimum value from the first derivative of magnetization versus temperature. T_C is ~ 5.0 K for $x = 0.08$, ~ 6.0 K for $x = 0.10$, ~ 7.0 K for $x = 0.12$, ~ 8.5 K for $x = 0.16$, and finally increases to ~ 10.0 K for $x = 0.20$. The maximum Curie temperature for $(Ca,Na)(Zn,Mn)_2Sb_2$ is three times lower than ~ 33 K for $(Ca,Na)(Zn,Mn)_2As_2$.[13] This may be because the lattice constants of $(Ca,Na)(Zn,Mn)_2Sb_2$ are larger than those of $(Ca,Na)(Zn,Mn)_2As_2$.[13] Similar trend has also been observed in $(Sr,Na)(Zn,Mn)_2As_2$, which has the hexagonal $CaAl_2Si_2$ structure and of which the lattice constant is between those of $(Ca,Na)(Zn,Mn)_2As_2$ and $(Ca,Na)(Zn,Mn)_2Sb_2$, has the maximum Curie temperature of ~ 24 K.[24] We use the Curie–Weiss formula $M = C/(T - \theta) + M_0$ to fit the curve above T_C, where θ is the Weiss temperature, C is a constant indicating the effective magnetic moment, and M_0 is a temperature-independent contribution. We plot the reverse of $M - M_0$ ver-

sus temperature in Fig. 3(c), and the linear fitting to data at high temperature intercept with x-axis is the Weiss temperature. The Weiss temperature θ is ~ 7.0 K for $x = 0.08$ and then increases to ~ 10.2 K for $x = 0.20$. We calculate the effective magnetic moment $M_{\rm eff}$ with $C = N\mu_0\mu_{\rm eff}^2/3k_{\rm B}$. The resultant $M_{\rm eff}$ is $\sim$4.49 $\mu_{\rm B}$/Mn, 4.41 $\mu_{\rm B}$/Mn, 4.67 $\mu_{\rm B}$/Mn, 4.03 $\mu_{\rm B}$/Mn, and 4.55 $\mu_{\rm B}$/Mn for $x = 0.08$, 0.10, 0.12, 0.16, and 0.20, respectively. These values are close to 5.9 $\mu_{\rm B}$ expected for Mn^{2+}, indicating that the Mn atoms in this material have a high spin state S = 5/2. The fitting data for $T_{\rm C}$, θ, and $M_{\rm eff}$ are tabulated in Table 1.

Table 1. The Curie temperature $T_{\rm C}$, Weiss temperature θ, effective moment $M_{\rm eff}$, and coercive field $H_{\rm C}$ for $(Ca_{1-x}Na_x)(Zn_{2-x}Mn_x)Sb_2$.

x	$T_{\rm C}$/K	θ/K	$M_{\rm eff}/(\mu_{\rm B}/{\rm Mn})$	$H_{\rm C}$/Oe
0.08	5.0	7.0	4.49	3
0.10	6.0	8.8	4.41	14
0.12	7.0	9.7	4.67	71
0.16	8.5	10.1	4.03	98
0.20	10.0	10.2	4.55	245

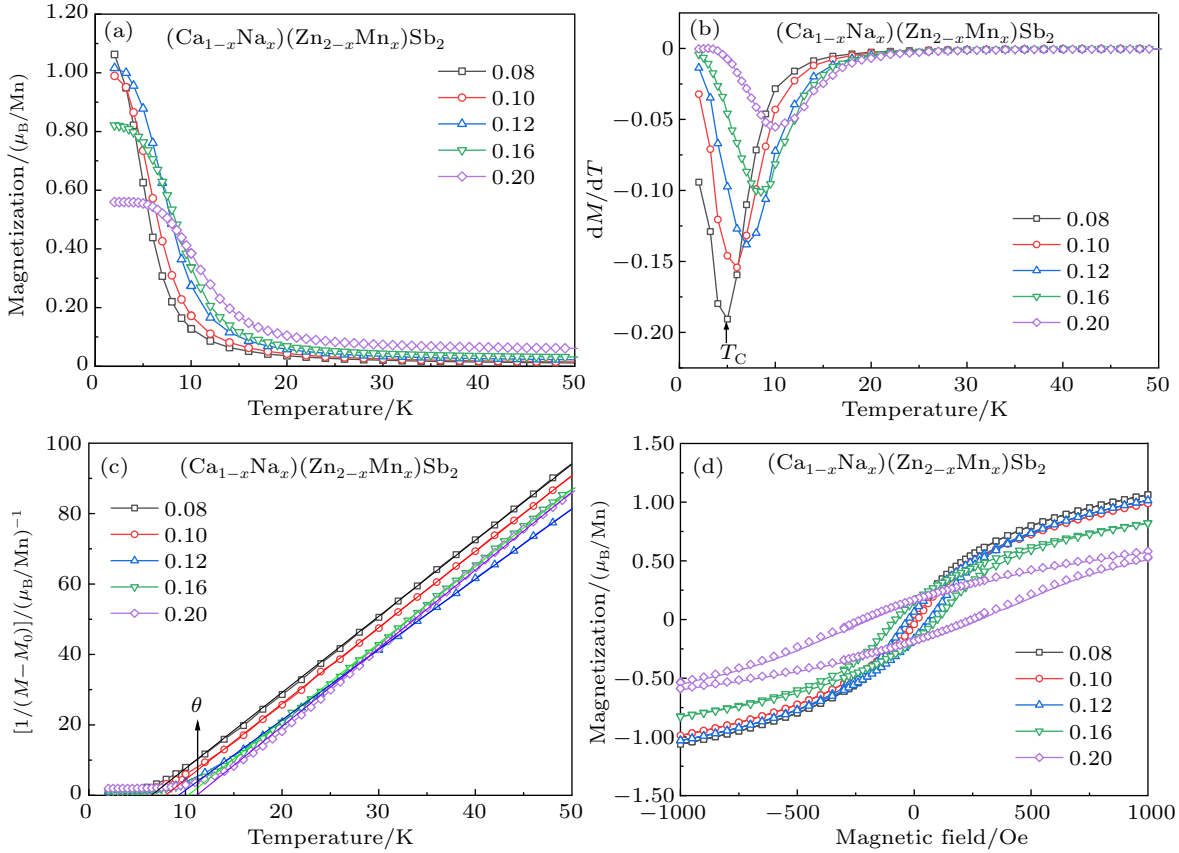


Fig. 3. (a) The temperature dependence of DC magnetization for $(Ca_{1-x}Na_x)(Zn_{2-x}Mn_x)Sb_2$ ($x = 0.08$, 0.10, 0.12, 0.16, 0.20) measured under field-cooling with external field of 1000 Oe. (b) The derivative of moment versus temperature for $(Ca_{1-x}Na_x)(Zn_{2-x}Mn_x)Sb_2$ ($x = 0.08$, 0.10, 0.12, 0.16, 0.20). The arrow marks the Curie temperature of $x = 0.08$. (c) The plot of $1/(M - M_0)$ versus temperature for $(Ca_{1-x}Na_x)(Zn_{2-x}Mn_x)Sb_2$ ($x = 0.08$, 0.10, 0.12, 0.16, 0.20). The arrow marks the Weiss temperature of $x = 0.20$. (d) Iso-thermal magnetization for $(Ca_{1-x}Na_x)(Zn_{2-x}Mn_x)Sb_2$ ($x = 0.08$, 0.10, 0.12, 0.16, 0.20) at 2 K.

In Fig. 3(d), we show the iso-thermal magnetization at 2 K for $(Ca_{1-x}Na_x)(Zn_{2-x}Mn_x)Sb_2$ ($x = 0.08$, 0.10, 0.12, 0.16, 0.20). Clear hysteresis loops can be observed in all samples, indicating that ferromagnetic ordering exists for all doping levels at 2 K. The coercive field $H_{\rm C}$ is ~ 3 Oe for $x = 0.08$, ~ 14 Oe for $x = 0.10$, ~ 71 Oe for $x = 0.12$, ~ 98 Oe for $x = 0.16$, and finally increases to ~ 245 Oe for $x = 0.20$. The increasing of the Curie temperature and coercive field with higher doping level is likely arising from the RKKY-like interaction of the Mn spins which are mediated by the hole carriers. Similar trend has been observed in other DMS materials that have been investigated by nuclear magnetic resonance and muon spin rotation experiments.[25,26] The $H_{\rm C}$ values are also tabulated in Table 1. The value is smaller than ~ 400 Oe for $(Ca,Na)(Zn,Mn)_2As_2$.[13]

In Fig. 4(a), we show the electrical resistivity of $(Ca_{1-x}Na_x)(Zn_{2-x}Mn_x)_2Sb_2$ ($x = 0.08$, 0.10, 0.12, 0.16, 0.20) down to 10 K. All samples display a metallic behavior. Besides, the resistivity increases monotonically from ~ 0.002 Ω·mm for $x = 0.08$ to ~ 0.008 Ω·mm for $x = 0.20$, indicating that doping more Mn atoms increases the probabilities of carriers been scattered by magnetic fluctuations. This behavior has also been observed in a 122-type DMS $(Sr,Na)(Cd,Mn)_2As_2$, which has the same $CaAl_2Si_2$ structure.[27]

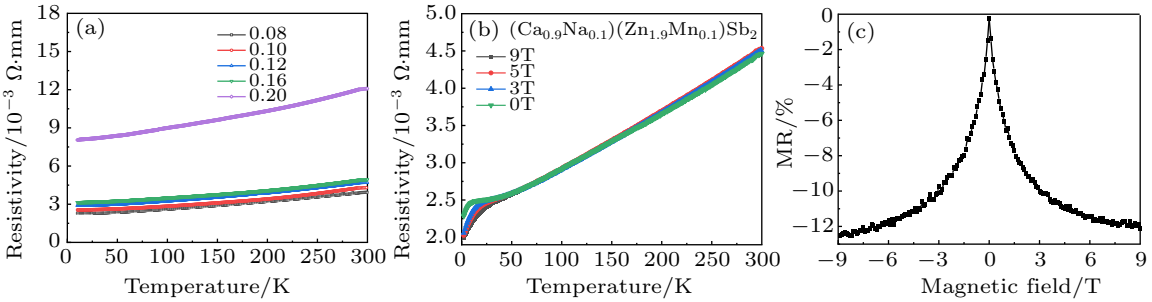


Fig. 4. (a) Resistivity for $(Ca_{1-x}Na_x)(Zn_{2-x}Mn_x)Sb_2$ ($x = 0.08$, 0.10, 0.12, 0.16, 0.20). (b) The magneto-resistance for $(Ca_{0.9}Na_{0.1})(Zn_{1.9}Mn_{0.1})Sb_2$ under the applied external magnetic fields of 0 T, 3 T, 5 T, 9 T. (c) The field dependence of MR for $(Ca_{0.9}Na_{0.1})(Zn_{1.9}Mn_{0.1})Sb_2$ from −9 T to 9 T at 2 K. The MR is defined as $[\rho_H - \rho_0]/\rho_0$.

In Fig. 4(b), we show the magneto-resistance (MR) of $(Ca_{0.9}Na_{0.1})(Zn_{1.9}Mn_{0.1})Sb_2$ measured under the applied external fields of 0 T, 3 T, 5 T, 9 T. The field dependent resistivity decreases below $T_C \sim 6$ K, indicating a negative magneto-resistance effect. This is due to the suppression of scattering of carriers by magnetic fluctuations under the external field. We plot the field dependence of MR for $(Ca_{0.9}Na_{0.1})(Zn_{1.9}Mn_{0.1})Sb_2$ from −9 T to 9 T at 2 K in Fig. 4(c). The MR is defined by the expression MR $= [\rho_H - \rho_0]/\rho_0$ and reaches 12% at 9 T. This value is comparable to MR = 8% for $(Ca,Na)(Zn,Mn)_2As_2$ at 7 T.[13]

4. Summary

To summarize, we turn nonmagnetic $CaZn_2Sb_2$ into ferromagnetic ordering by doping Na and Mn into $CaZn_2Sb_2$. Na provides carriers and Mn provides local moments, respectively. A new DMS material $(Ca,Na)(Zn,Mn)_2Sb_2$ with Curie temperature $T_C \sim 10$ K has been successfully synthesized. Isothermal magnetization measurements show that the coercive field is ∼ 245 Oe. Further more, this material shows a negative magneto-resistance with MR ∼ 12%. This new ferromagnetic semiconductor stands as a new member in novel DMS families with decoupled charge and spin dopings, and provides a new choice to develop junctions with the same $CaAl_2Si_2$ structure of iron-based superconductors and other antiferromagnets.

Note added During the preparation of this manuscript, we became aware of the same material $(Ca,Na)(Zn,Mn)_2Sb_2$ has just been published in *Physical Review Materials* by Yu *et al.*[28] The results in our independent work are quantitatively consistent to theirs.

References

[1] Ohno H, Shen A, Matsukura F, Oiwa A, Endo A, Katsumoto S and Iye Y 1996 *Appl. Phys. Lett.* **69** 363
[2] Dietl T 2010 *Nat. Mater.* **9** 965
[3] Ohno H 1998 *Science* **281** 951
[4] Zutic I, Fabian J and Sarma S D 2004 *Rev. Mod. Phys.* **76** 323
[5] Dietl T, Ohno H, Matsukura F, Cibert J and Ferrand D 2000 *Science* **287** 1019
[6] Chen L, Yang X, Yang F, Zhao J, Misuraca J, Xiong P and von Molnar S 2011 *Nano Lett.* **11** 2584
[7] Ding C and Ning F L 2014 *Sci. Sin-Phys. Mech. Astron.* **44** 1140
[8] Guo S L and Ning F L 2018 *Chin. Phys. B* **27** 097502
[9] Gu Y L, Guo S L and Ning F L 2019 *J. Semicond.* **40** 081506
[10] Deng Z, Jin C Q, Liu Q Q, Wang X C, Zhu J L, Feng S M, Chen L C, Yu R C, Arguello C and Goko T 2011 *Nat. Commun.* **2** 422
[11] Deng Z, Zhao K, Gu B, Han W, Zhu J L, Wang X C, Li X, Liu Q Q, Yu R C, Goko T, Frandsen B, Liu L, Zhang J S, Wang Y Y, Ning F L, Maekawa S, Uemura Y J and Jin C Q 2013 *Phys. Rev. B* **88** 081203
[12] Zhao K, Deng Z, Wang X C, Han W, Zhu J L, Li X, Liu Q Q, Yu R C, Goko T, Frandsen B, Liu L, Ning F L, Uemura Y J, Dabkowska H, Luke G M, Luetkens H, Morenzoni E, Dunsiger S R, Senyshyn A, Boni P and Jin C Q 2013 *Nat. Commun.* **4** 1442
[13] Zhao K, Chen B J, Deng Z, Han W, Zhao G Q, Zhu J L, Liu Q Q, Wang X C, Frandsen B, Liu L, Cheung S, Ning F L, Munsie T J S, Medina T, Luke G M, Carlo J P, Munevar J, Zhang G M, Uemura Y J and Jin C Q 2014 *J. Appl. Phys.* **116** 163906
[14] Ding C, Man H Y, Qin C, Lu J C, Sun Y L, Wang Q, Yu B Q, Feng C M, Goko T, Arguello C J, Liu L, Frandsen B A, Uemura Y J, Wang H D, Luetkens H, Morenzoni E, Han W, Jin C Q, Munsie T, Williams T J, D Ortenzio R M, Medina T, Luke G M, Imai T and Ning F L 2013 *Phys. Rev. B* **88** 041102
[15] Lu J C, Man H Y, Ding C, Wang Q, Yu B Q, Guo S L, Wang H D, Chen B, Han W, Jin C Q, Uemura Y J and Ning F L 2013 *EPL* **103** 67011
[16] Zhao Y, Wang K, Guo S L, Fu, L C, Gu Y L, Zhi G X, Xu L X, Cui Q, Cheng J G, Wang H D, Chen B and Ning F L 2017 *EPL* **120** 47005
[17] Dunsiger S R, Carlo J P, Goko T, Nieuwenhuys G, Prokscha T, Suter A, Morenzoni E, Chiba D, Nishitani Y, Tanikawa T, Matsukura F, Ohno H, Ohe J, Maekawa S and Uemura Y J 2010 *Nat. Mater.* **9** 299
[18] Ning F L, Man H Y, Gong X, Zhi G X, Guo S L, Ding C, Wang Q, Goko T, Liu L, Frandsen B A, Uemura Y J, Luetkens H, Morenzoni E, Jin C Q, Munsie T, Luke G M, Wang H D and Chen B 2014 *Phys. Rev. B* **90** 085123
[19] Zhao K, Chen B J, Zhao G Q, Yuan Z, Liu Q Q, Deng Z, Zhu J L and Jin C Q 2014 *Chin. Sci. Bull.* **59** 2524
[20] Guo S L, Man H Y, Wang K, Ding C, Zhao Y, Fu L C, Gu Y L, Zhi G X, Frandsen B A, Cheung S C, Guguchia Z, Yamakawa K, Chen B, Wang H, Deng Z, Jin C Q, Uemura Y J and Ning F L 2019 *Phys. Rev. B* **99** 155201
[21] Guo S L, Man H Y, Gong X, Ding C, Zhao Y, Chen B, Guo, Y, Wang H D and Ning F L 2016 *J. Magn. Magn. Mater.* **400** 295
[22] May A F, Mcguire M A, Ma J, Delaire O, Huq A and Custelcean R 2012 *J. Appl. Phys.* **111** 033708
[23] Toby B H and Von Dreele R B 2013 *J. Appl. Crystallogr.* **46** 544
[24] Chen B J, Zhao K, Deng Z, Han W, Zhu J L, Wang X C, Liu Q Q, Frandsen B, Liu L, Cheung S, Ning F L, Munsie T J S, Medina T, Luke G M, Carlo J P, Munevar J, Uemura Y J and Jin C Q 2014 *Phys. Rev. B* **90** 155202
[25] Ding C, Qing C, Man H Y, Imai T and Ning F L 2013 *Phys. Rev. B* **88** 041108
[26] Sun F, Li N N, Chen B J, Jia Y T, Zhang L J, Li W M, Zhao G Q, Xing L Y, Fabbris G, Wang Y G, Deng Z, Uemura Y J, Mao H K, Haskel D, Yang W G and Jin C Q 2016 *Phys. Rev. B* **93** 224403
[27] Chen B J, Deng Z, Li W M, Gao M R, Li Z, Zhao G Q, Yu S, Wang X C, Liu Q Q and Jin C Q 2016 *J. Appl. Phys.* **120** 083902
[28] Yu S, Liu X Y, Zhao G Q, Peng Y, Wang X C, Zhao J F, Li W M, Deng Z, Furdyna J K, Uemura Y J and Jin C Q 2020 *Phys. Rev. Mater.* **4** 024411